# Variable Procedural Strategies Adapted to Anatomical Characteristics in Catheter Ablation of the Cavotricuspid Isthmus Using a Preoperative Multidetector Computed Tomography Analysis

KENTA KAJIHARA, M.D.,* YUKIKO NAKANO, M.D., PH.D.,* YUKOH HIRAI, M.D., PH.D.,* HIROSHI OGI, M.D., PH.D.,* NOBORU ODA, M.D., PH.D.,* KAZUYOSHI SUENARI, M.D., PH.D.,* YUKO MAKITA, M.D.,* AKINORI SAIRAKU, M.D.,* TAKEHITO TOKUYAMA, M.D.,* CHIKAAKI MOTODA, M.D.,* MAI FUJIWARA, M.D.,* YOSHIKAZU WATANABE, M.D.,* MASAO KIGUCHI, R.T.,† and YASUKI KIHARA, M.D., PH.D.*

From the *Department of Cardiovascular Medicine, Graduate School of Biomedical and Health Sciences; and †Department of Radiology, Hiroshima University Hospital, Hiroshima, Japan

**Variable Strategies for CTI Ablation.** ***Objectives:*** **This study aimed to investigate the anatomical characteristics complicating cavotricuspid isthmus (CTI) ablation and the effectiveness of various procedural strategies.**

***Methods and Results:*** **This study included 446 consecutive patients (362 males; mean age 60.5 ± 10.4 years) in whom CTI ablation was performed. A total of 80 consecutive patients were evaluated in a preliminary study. The anatomy of the CTI was evaluated by multidetector row-computed tomography (MDCT) prior to the procedure. A multivariate logistic regression analysis revealed that the angle and mean wall thickness of the CTI, a concave CTI morphology, and a prominent Eustachian ridge, were associated with a difficult CTI ablation ($P < 0.01$). In the main study, 366 consecutive patients were divided into 2 groups: a modulation group (catheter inversion technique for a concave aspect, prominent Eustachian ridge, and steep angle of the CTI or increased output for a thicker CTI) and nonmodulation group (conventional strategy). The duration and total amount of radiofrequency energy delivered were significantly shorter and smaller in the modulation group than those in the nonmodulation group (162.2 ± 153.5 vs 222.7 ± 191.9 seconds, $P < 0.01$, and 16,962.4 ± 11,545.6 vs 24,908.5 ± 22,804.2 J, $P < 0.01$, respectively). The recurrence rate of type 1 atrial flutter after the CTI ablation in the nonmodulation group was significantly higher than that in the modulation group (6.3 vs 1.7%, $P = 0.02$).**

***Conclusion:*** **Changing the procedural strategies by adaptating them to the anatomical characteristics improved the outcomes of the CTI ablation.** *(J Cardiovasc Electrophysiol, Vol. 24, pp. 1344-1351, December 2013)*

*atrial flutter, catheter ablation, cavotricuspid isthmus, eustachian ridge, multidetector row-computed tomography*

## Introduction

The cavotricuspid isthmus (CTI) is defined as the area between the tricuspid valve (TV) and inferior vena cava (IVC), and is contiguous in anatomy to the triangle of Koch. The CTI is a critical component of the reentry circuit for CTI-dependent atrial flutter (AFL).[1-5] Radiofrequency (RF) catheter ablation targeting the CTI is the optimal treatment for CTI-dependent AFL.[6,7] Despite high overall success rates, the ablation procedure is occasionally difficult due to variations in the anatomical characteristics of the CTI.[8,9] Multidetector row-computed tomography (MDCT) has become a widely used substitute in cardiac angiography studies.[10]

In a preliminary study, the CTI anatomy was evaluated using 64-row MDCT, and the anatomical characteristics of the CTI that complicate the ablation procedure were identified. Subsequently, adaptations to the CTI ablation strategies according to the anatomical information provided by the preprocedural MDCT were prospectively examined in a main study. The goal was to improve and minimize the difficulty of the ablation procedure.

## Methods

### *Study Subjects*

The institutional review board approved the study, and written informed consent was obtained from all patients. Patients with a serum creatinine level of 1.2 mg/dL or more were excluded from the study. Patients in which adequate anatomical information necessary to perform the measurements was not obtained during the MDCT scan were

No disclosures.

Address for correspondence: Kenta Kajihara, M.D., Department of Cardiovascular Medicine, Hiroshima University Graduate School of Biomedical and Health Sciences, 1-2-3 Kasumi, Minami-ku, Hiroshima 734-8551, Japan. Fax: +81-82-257-5169; E-mail: g5u6g27@yahoo.co.jp

Manuscript received 20 April 2013; Revised manuscript received 14 June 2013; Accepted for publication 26 June 2013.

doi: 10.1111/jce.12231

excluded. Fortunately, the scans in all subjects provided the necessary anatomical information and it was not necessary to exclude any subjects due to an uninterpretable scan quality.

### *Preliminary Study*

In total, 80 patients (63 males [79.7%], aged 59.8 ± 10.4 years) in whom CTI ablation was successfully performed using an 8 mm tip ablation catheter were included from the preliminary study. MDCT was performed within 24 hours before the ablation procedure in all patients. Typical AFL was clinically documented in 23 patients (AFL only: n = 7; both atrial fibrillation (AF) and AFL: n = 16). The remaining 57 patients with persistent or paroxysmal AF underwent a combined AF and CTI ablation with no evidence of AFL. Of the 73 patients with AF in whom circumferential pulmonary vein isolation (CPVI) was performed, paroxysmal AF was evident in 63 patients and persistent AF in 10.

### *Main Study*

Three hundred and sixteen consecutive patients (males: n = 255, 80.7%, aged 60.5 ± 10.2 years) scheduled for a CTI ablation were prospectively enrolled in the main study. Typical AFL was clinically documented in 22 patients. In the remaining 294 patients (including 56 patients with AFL) with persistent or paroxysmal AF, a combined AF and CTI ablation was performed with no evidence of AFL.

### *Multidetector Computed Tomography Protocol and Image Reconstruction*

MDCT data sets were acquired using a 64-slice CT scanner (Lightspeed VCT; GE Healthcare, Waukesha, WI, USA) with retrospective ECG-gated scans using a dual-shot-type injector (Nemoto-Kyorindo, Tokyo). To satisfy these conflicting issues, we used a multiphasic contrast material injection protocol. In the routine protocol, the first phase of the multistepwise protocol, 144 mgI/kg were administered during 7 seconds. In the second phase, the initial contrast concentration was 370 mgI/mL; it was gradually decreased by dilution with saline during 15 seconds. The total iodine dose in the second phase was 155 mg/kg. The scan protocol methods used in this study have been described previously.[11] Image analysis software (Virtual Place Advance; AZE, Tokyo, Japan) allowed 3-dimensional (3D) viewing of multiplanar reconstruction images reformatted as cross-sectional images. The optimal image was selected during the end-diastole phase of the right atrium, which was defined as the image immediately before the opening of the tricuspid valve. The images were also reconstructed using electrocardiography (ECG) edited at the level of the anomalies of the ECG signal, which were caused by premature beats, AF, and mistriggering. Multiplanar reconstructions of the axial images were obtained by operating a cursor manually on selected cross-sectional source images orthogonal to the source images during the latest right atrial diastolic phase of the cardiac cycle [30–40% of the interbeat (R–R) interval].

### *Measurements of the Anatomical Parameters of the Cavotricuspid Isthmus*

The quantative measurements and morphologies of the CTI were analyzed in all patients. The values for the length (Fig. 1A) and angle (Fig. 1B) were obtained in long-axis 2-chamber right anterior oblique views parallel to the septum. The length of the CTI was defined as the segment beginning from the base of the end of the Eustachian valve to the base of the tricuspid valve. The angle was constructed by the intersection of the line passing through the center of the IVC and the line extending to the orifice of the IVC from the tricuspid annulus. The presence of a prominent Eustachian ridge was confirmed in the same view. The myocardial thickness of the CTI was measured at the center of the 3 parallel isthmic levels (paraseptal, central, and inferolateral) in the short-axis left anterior oblique views (Fig. 1C,D). The mean myocardial thickness of the CTI was calculated from the values of those 3 sites. The angle of the CTI was classified into 2 types (steep: $<90^\circ$ and gentle: $\geq 90^\circ$). The CTI morphology was classified into 3 types; straight ($\leq$3 mm), concave (>3 to $\leq$5 mm), and pouchlike (>5 mm), according to the depth of the CTI.[10] Also, the analysis software of this study could measure only to the first decimal place. Two blinded cardiologists experienced in reading MDCT images independently analyzed all the data sets. Quantitative measurements were performed in triplicate.

### *Electrophysiological Study and Catheter Ablation*

Continuous monitoring was performed using endocardial electrocardiography (bandpass filtered 30–500 Hz) and surface electrocardiography. Data were stored on a digital amplifier and recorder system (Bard Electrophysiology, Lowell, MA, USA). A 6F multipolar (15-pole) catheter (Irvine Biomedical, Irvine, CA, USA) was utilized with the distal poles (poles 1−10) placed within the coronary sinus (CS) and the proximal electrodes (poles 11−15) located from the superior vena cava to the superior right atrium via the right internal jugular vein. A decapolar electrode catheter was positioned on the lateral wall of the right atrium (Irvine Biomedical) inserted from the right femoral vein. A decapolar electrode catheter (Biosense Webster, Diamond Bar, CA, USA) was introduced via the femoral vein into the region of the bundle of His.

After intravenous administration of heparin (bolus injection of 3000 IU followed by an hourly injection of 1000 IU), a 7F quadripolar deflectable catheter with an 8 mm tip electrode (Navister; Biosense Webster) was positioned on the isthmus using a preshaped long sheath with a $180^\circ$ curve (RAMP curve, St. Jude Medical, Daig Division, Inc., Minnetonka, MN, USA). In the beginning, the ablation catheter was positioned at the ventricular aspect of the CTI at the 6 o'clock position in the LAO $45^\circ$ projection. Ablation was carried out with the temperature set at 55 °C and energy output at 40−50 W using a dragging catheter technique under anatomic and electrographic guidance.[4,12,13] RF was applied with voltage outputs modulated by impedance monitoring to avoid an increase due to excessive heating.[14] Ablation of the CTI was performed during either sinus rhythm (pacing from the CS) or ongoing typical AFL with the procedural endpoint of complete bidirectional isthmus block.[15] Reversal of the right atrial depolarization sequence was established by a complete CTI map using a decapolar mapping catheter straddling the line of block and by recording widely separated (>120 milliseconds) local double potentials along the ablation line during atrial pacing.[16] Differential pacing was performed to distinguish complete from incomplete bidirectional isthmus block. When complete conduction block of

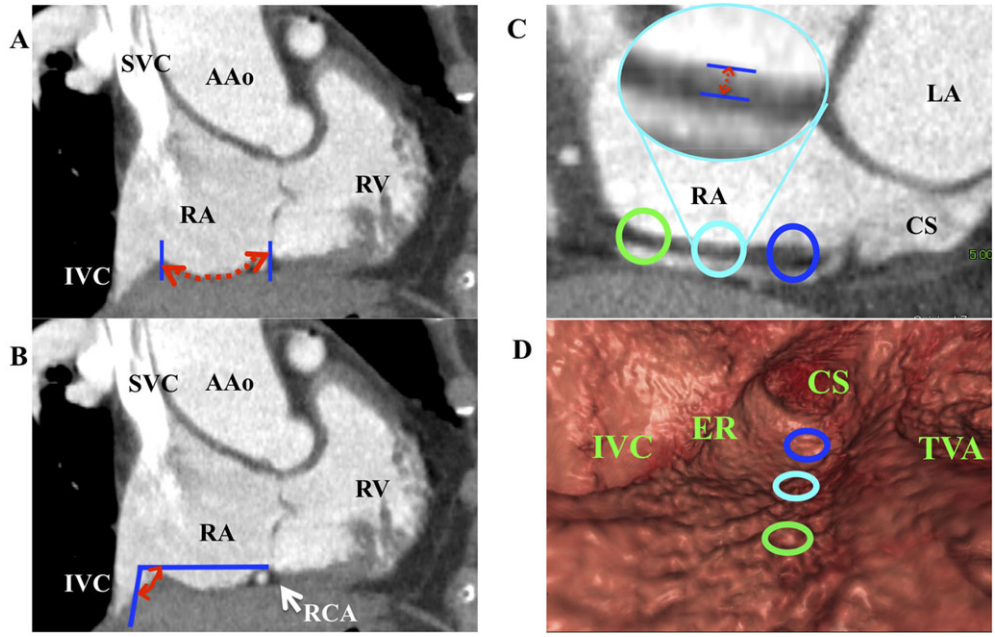


**Figure 1.** *Quantitative measurements and morphologies of the CTI. Values for the length and angle were obtained in the long-axis 2-chamber right anterior oblique views parallel to the septum. Panel A: The length of the CTI (red double-headed arrow) was defined as the segment beginning from the base of the end of the Eustachian valve to the base of the tricuspid valve. Panel B: The angle (red curve line) was constructed by the intersection of the line passing through the center of the IVC and a line extended to the orifice of the IVC from the tricuspid annulus. Panels C and D: The myocardial thickness of the CTI was measured at the center of 3 parallel isthmic levels in the short-axis left anterior oblique view (paraseptal; blue circle, central; light blue, and inferolateral; light green). The wall thickness, manually measured on an image, took into account the visually detectable wall edges (spread light blue circle). Panel D shows the virtual endoscopic view of the right atrium around the CTI.*

the CTI was not achieved after first-line ablation, the conduction gaps were mapped and ablated searching for single or narrow-split potentials with the ablation catheter moving along the original ablation line. If conduction block was not still achieved, the catheter was repositioned on the ventricular side of the CTI at the 7 or 5 o'clock position. If bidirectional block status was maintained over the 30-minute period following the achievement of the bidirectional block, the procedure was considered complete.

In this study, the procedure time of the CTI ablation was defined as the duration from the beginning of the first RF application to confirmation of the bidirectional block of the CTI, excluding the observation time. The CTI was divided into a proximal part (from the coronary sinus ostium to the Eustachian valve) and a distal part (from the tricuspid annulus to the coronary sinus ostium) according to a catheter placed within the CS. The region in which a complete bidirectional conduction block was successfully achieved was recorded. For patients in whom a combined AF and CTI ablation was performed, CPVI was performed at the beginning of the procedure. The patients were mildly sedated without intubation during the procedure using short acting intravenous drugs.

### *Ablation Protocol of the Main Study*

The patients were prospectively randomized and assigned to either a modulation or nonmodulation group. In the modulation group (n = 183), the ablation strategies were modulated according to a flow chart that was based on the results of the preliminary study (Fig. 2). In brief, if the thickness of the CTI was $\geq$2.7 mm, the CTI ablation was initiated with a high output (60 W) and high-temperature (60 °C) setting from the beginning. If the morphology of the CTI was concave, angle of the CTI was $\leq$86.4°, or a prominent Eustachian ridge was found, the catheter was inverted until the outer curve was in contact with the isthmus at the proximal part of the CTI (Fig. 3). Thus, the catheter came in contact with the outer surface of the CTI in these cases. In the absence of any of these anatomical features, the CTI ablation was performed by the conventional method. In the nonmodulation group (n = 183), the ablation lines were created conventionally, similar to the method in the preliminary study. Verification of the bidirectional block in the CTI was also performed as in the preliminary study.

### *Patient Follow-Up*

The patients were examined in our outpatient clinic 2 weeks after performance of the ablation procedure. Follow-up continued every 1−2 months thereafter. Patients were examined using 12-lead ECG and Holter monitoring. Interviews were conducted regarding clinical symptoms and residual palpitations.

### *Statistical Analysis*

The data were tested for normal (Gaussian) distribution using the Kolmogorov−Smirnov test. Normally distributed continuous variables are presented as means ± SD. In the case of a non-Gaussian distribution, median values and quartiles are given. Comparisons between groups were performed using Student's *t*-test. In cases of continuous data with a non-Gaussian distribution, the Mann−Whitney U test was used. Categorical variables were compared using the Fisher's exact test. A univariate analysis of the patient characteristics was conducted for a comparison between the difficult and

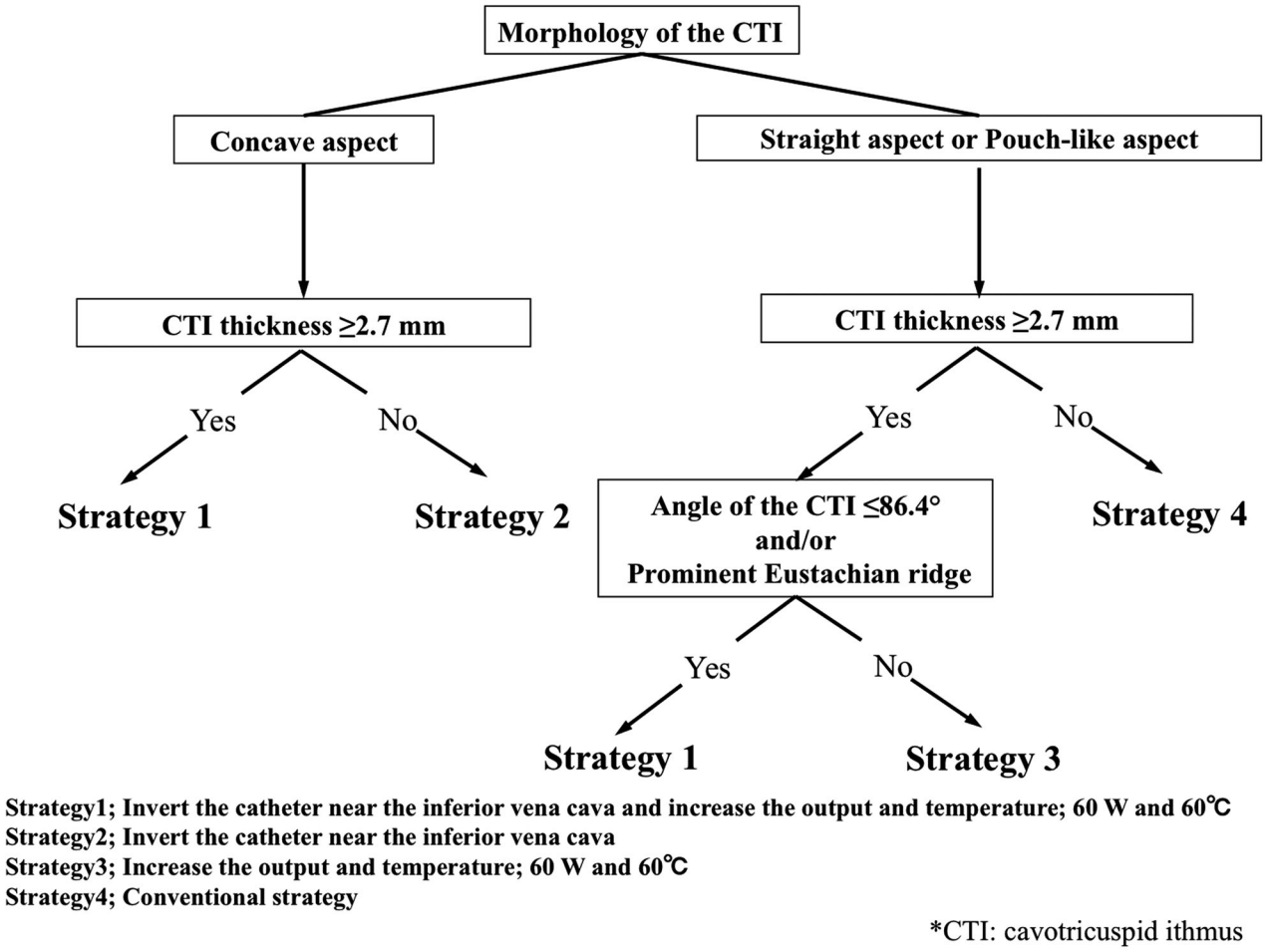


**Figure 2.** *Flow chart of the ablation strategies in the modulation group. The ablation strategies were modulated according to this flow chart in the modulation group.*

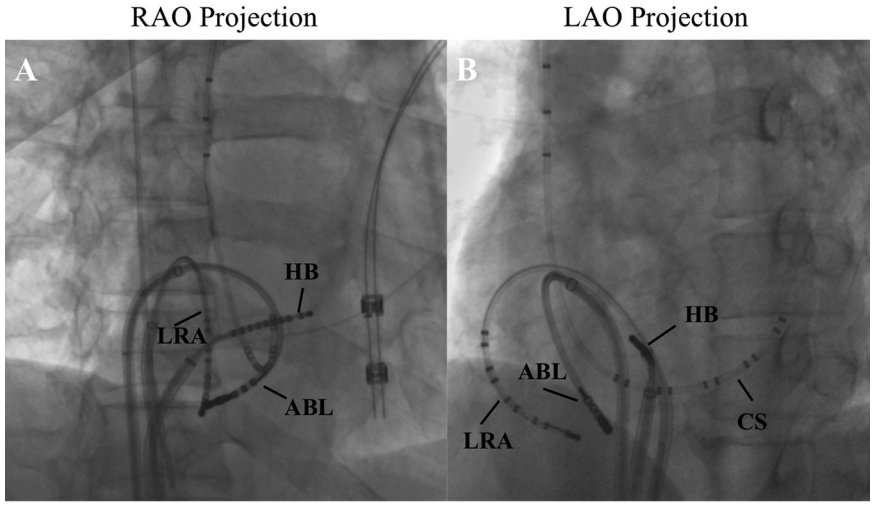


**Figure 3.** *Catheter inversion technique. Radiographs in the right anterior oblique (RAO; A) and left anterior oblique (LAO; B) projections show the inverted ablation catheter (ABL) within the right atrium targeting the region of the Eustachian ridge. ABL = an 8 mm tipped ablation catheter; CS = a decapolar catheter positioned in the proximal coronary sinus; HB = a decapolar catheter in the region of the His-bundle; LRA = a decapolar circular catheter in the lateral right atrium.*

straightforward cases, and a logistic regression analysis was performed to detect any independent significant predictors by adjusting for multiple variables. The multiple pairwise comparisons among the patient groups were tested using a Tukey–Kramer test for continuous variables. Statistical significance was defined as a $P < 0.05$ using a 2-sided comparison. Statistical analyses were performed using JMP 9 software (SAS Software, Cary, NC, USA).

## Results

### *Preliminary Study*

The baseline characteristics of the 80 subjects and ablation results of the preliminary study are summarized in Table 1. For the myocardial thickness of the CTI, there was no significant difference between the 3 parallel isthmic levels

**TABLE 1**
Patient Characteristics and Ablation Results of the Preliminary Study

| Parameters | Results (n = 80) |
|---|---|
| **Patient characteristics** | |
| Gender male, n (%) | 63 (79.7) |
| Age, year | 59.8 ± 10.4 |
| BMI, kg/m$^2$ | 23.9 ± 2.9 |
| Left ventricular ejection fraction, % | 64.0 ± 9.9 |
| Hypertrophic cardiomyopathy, n (%) | 2 (2.5) |
| Dilated cardiomyopathy, n (%) | 1 (1.2) |
| Coronary artery disease, n (%) | 4 (5.0) |
| Valvular heart disease, n (%) | 4 (5.0) |
| **Anatomical data collected from MDCT** | |
| Length of the CTI, mm | 29.9 ± 7.6 |
| Angle of the CTI, degree | 97.6 ± 26.7 |
| Angle type of the CTI | |
| Steep type, n (%) | 16 (20.0) |
| Gentle type, n (%) | 64 (80.0) |
| Mean thickness of the CTI, mm | 2.5 ± 0.6 |
| Prominent Eustachian ridge, n (%) | 11 (13.8) |
| Morphology of the CTI | |
| Straight aspect, n (%) | 46 (57.5) |
| Concave aspect, n (%) | 20 (25.0) |
| Pouch-like aspect, n (%) | 14 (17.5) |
| **Ablation results** | |
| Ablation during AFL, n (%) | 3 (3.8) |
| Procedure time, minutes | 21.8 ± 20.9 |
| Total RF application duration, seconds | 346.4 ± 321.4 |
| Total RF energy, J | 26,482.5 ± 21,403.4 |
| Fluoroscpic time, minutes | 13.1 ± 11.8 |

AFL = atrial flutter; BMI = body mass index; CTI = cavotricuspid isthmus; MDCT = multidetecter computed tomography; RF = radiofrequency.

(paraseptal: 2.61 ± 0.46 vs central: 2.41 ± 0.51 vs inferolateral: 2.38 ± 0.43) by Tukey–Kramer multiple comparison tests. Bidirectional conduction block in the CTI was achieved in all patients. The subjects in the preliminary study were divided into 2 groups according to the median procedure time: the difficult cases (n = 40; procedure time ≥16 minutes) and straightforward cases (n = 40; procedure time <16 minutes).

A multivariate logistic regression analysis revealed that the mean thickness of the CTI, steep angle of the CTI, concave aspect of the CTI morphology, and prominent Eustachian ridge were characteristics significantly associated with the difficulty of the CTI ablation (Table 2).

The area under the curve was 0.73 ($P < 0.01$) for the angle of the CTI and 0.95 ($P < 0.01$) for the thickness of the CTI. The optimal cutoff values according to this analysis were 86.4° for the angle of the CTI (sensitivity: 55%, specificity: 90%) and 2.67 mm for the thickness of the CTI (sensitivity: 92.5%, specificity: 87.5%). These values were useful in predicting the procedural difficulty of the CTI ablation.

The procedure time of the CTI ablation was significantly longer in the patients whose critical point for a successful ablation was the proximal part than that in the patients whose critical point of a successful ablation was the distal part ($P < 0.05$). Especially in terms of the variations in the anatomical characteristics of the CTI including a concave aspect (38.7 ± 35.0 vs 17.5 ± 15.3 minutes, $P = 0.02$), prominent Eustachian ridge (27.4 ± 19.7 vs 9.1 ± 7.7 minutes, $P = 0.04$), and steep angle of the CTI (57.5 ± 32.1 vs 30.7 ± 14.2 minutes, $P = 0.02$), achievement of bidirectional isthmus block in the proximal part was significantly more difficult than that of the distal part.

### *Efficacy of Varying the Procedural Strategies According to the Cavotricuspid Isthmus Anatomy*

In this prospective, randomized study, no significant difference was evident in the baseline and anatomical characteristics between the nonmodulation and modulation groups (Table 3). In the results of the CTI ablation in both groups (Table 3), the total CTI ablation procedure time was significantly shorter in the modulation group than that in the nonmodulation group. Further, the total RF duration was significantly shorter and total amount of RF energy required to establish bidirectional conduction block at the CTI was significantly smaller in the modulation group than that in the nonmodulation group. In addition, the fluoroscopic time was significantly shorter in the modulation group than that in the nonmodulation group. The results of the comparison of the procedure time between the modulation and nonmodulation groups according to the anatomical characteristics complicating the CTI ablation are shown in Fig. 4. Tukey–Kramer tests revealed that the procedure time in the patients with a concave aspect, thickness of the CTI ≥2.7 mm, angle of the CTI ≤86.4° or prominent Eustachian ridge was significantly longer than that in those without in the nonmodulation group (30.4 ± 23.6, 31.6 ± 23.6, 41.2 ± 26.5, 52.6 ± 37.3 vs 9.1 ± 6.8 minutes, $P < 0.05$). However, in the modulation group, there was no significant difference in the procedure time between the patients with anatomical difficulty and those without (13.6 ± 8.5, 12.8 ± 9.2, 13.2 ± 9.4, 12.4 ± 8.6 vs 9.3 ± 8.2 minutes).

### *Follow-Up Results*

During the 28.8 ± 12.5 months follow-up periods, the recurrence rate of type 1 AFL after the CTI ablation in the nonmodulation group was significantly higher than that in the modulation group (6.3 vs 1.7%, $P = 0.02$).

## Discussion

### *Major Findings*

In this study, we first identified the anatomical characteristics of the CTI that caused difficulty in the ablation procedure by analyzing the preprocedural MDCT images. Those were the angle and mean wall thickness of the CTI, a concave CTI morphology, and a prominent Eustachian ridge. We continuously demonstrated that changing the ablation strategy based on the anatomical information of the CTI by the analysis MDCT data improved the CTI ablation procedure, especially in the difficult cases.

### *Comparison with Previous Studies*

Knecht *et al*. reported the thickness of the CTI as an anatomic parameter strongly associated with procedural difficulty in the achievement of transmural lesions[9] similar to the results of our study. Heidbüchel *et al*. noted that the presence of a Eustachian ridge (valve) and a concave aspect was associated with a significantly higher number of RF applications to achieve conduction block of the CTI.[8] Catheter inversion may improve the catheter contact in these cases. Sporton *et al*. and Wieczorek *et al*. reported that untreated single electrograms could be identified predominantly in the proximal portions of the CTI following the inversion of

**TABLE 2**

Univariate and Multivariate Logistic Regression Analyses of the Anatomical Difficulty of CTI Ablation

| Variables | Univariate Odds Ratio (95% Confidence Interval) | *P* Value | Multivariate Odds Ratio (95% Confidence Interval) | *P* Value |
|---|---|---|---|---|
| Age, per year | 1.00 (0.97–1.03) | 0.96 | 0.99 (0.94–1.04) | 0.75 |
| Male sex | 1.69 (0.71–4.14) | 0.24 | 1.30 (0.35–4.73) | 0.69 |
| BMI, per kg/m$^2$ | 1.01 (0.90–1.16) | 0.75 | 1.04 (0.87–1.27) | 0.62 |
| Length of the CTI, per mm | 1.04 (0.99–1.09) | 0.15 | 1.05 (0.97–1.11) | 0.31 |
| Mean thickness of the CTI, per mm | 6.35 (2.67–16.68) | <0.01 | 7.10 (2.39–24.45) | <0.01 |
| Steep angle of the CTI | 8.5 (2.64–38.11) | <0.01 | 11.47 (2.65–66.21) | <0.01 |
| Straight aspect | 0.42 (0.20–0.86) | 0.02 | 2.52 (0.24–33.56) | 0.45 |
| Concave aspect | 5.79 (2.49–14.57) | <0.01 | 24.56 (2.21–419.32) | <0.01 |
| Pouch-like aspect | 0.57 (0.21–1.46) | 0.24 | 2.59 (0.20–36.34) | 0.47 |
| Prominent Eustachian ridge | 18.31 (3.45–338.75) | <0.01 | 37.42 (5.45–790.63) | <0.01 |

BMI = body mass index; CTI = cavotricuspid isthmus.
All the variables in the columns were used in the multivariate model.

**TABLE 3**

Patient Characteristics and Ablation Results of the Nonmodulation and Modulation Groups

| Variables | Modulation Group (n = 183) | Nonmodulation Group (n = 183) | *P* Value |
|---|---|---|---|
| **Patient characteristics** | | | |
| Gender male, n (%) | 152 (83.1) | 147 (80.3) | 0.50 |
| Age, years* | 60.9 ± 10.4 | 60.3 ± 10.3 | 0.61 |
| BMI, kg/m$^{2*}$ | 24.2 ± 3.0 | 24.2 ± 3.2 | 0.81 |
| Left ventricular ejection fraction, %* | 61.9 ± 6.1 | 61.5 ± 5.8 | 0.51 |
| Hypertrophic cardiomyopathy, n (%) | 2 (1.1) | 1 (0.6) | 0.56 |
| Dilated cardiomyopathy, n (%) | 1 (0.6) | 1 (0.6) | 1.00 |
| Coronary artery disease, n (%) | 3 (1.6) | 4 (2.2) | 0.70 |
| Valvular heart disease, n (%) | 8 (4.4) | 7 (3.8) | 0.79 |
| **Anatomical data collected from MDCT** | | | |
| Length of the CTI, mm* | 31.9 ± 8.0 | 32.3 ± 7.3 | 0.93 |
| Angle of the CTI, degree* | 104.1 ± 22.5 | 101.3 ± 21.4 | 0.22 |
| Angle type of the CTI | | | |
| Steep type, n (%) | 34 (18.6) | 32 (17.5) | 0.79 |
| Gentle type, n (%) | 149 (81.4) | 151 (18.5) | 0.79 |
| Mean thickness of the CTI, mm* | 2.6 ± 0.3 | 2.6 ± 0.5 | 0.27 |
| Morphology of the CTI | | | |
| Straight aspect, n (%) | 105 (57.4) | 111 (60.7) | 0.52 |
| Concave aspect, n (%) | 48 (26.2) | 50 (27.3) | 0.81 |
| Pouch-like aspect, n (%) | 30 (16.4) | 22 (12.0) | 0.23 |
| Prominent Eustachian ridge, n (%) | 15 (8.2) | 20 (10.9) | 0.37 |
| Thickness of the CTI ≥2.7 mm, n (%) | 58 (31.7) | 62 (33.9) | 0.66 |
| Angle of the CTI ≤86.4, n (%) | 30 (16.4) | 28 (15.3) | 0.77 |
| **Ablation results** | | | |
| Ablation during AFL, n (%) | 8 (4.4) | 10 (5.5) | 0.63 |
| Procedure time, minutes* | 10.0 ± 8.7 | 18.1 ± 17.8 | <0.01 |
| Total RF application duration, seconds* | 166.2 ± 153.5 | 222.7 ± 191.9 | <0.01 |
| Total RF energy, J* | 16,962.4 ± 11,545.6 | 24,908.5 ± 22,804.2 | <0.01 |
| Fluoroscpic time, minutes* | 6.8 ± 5.7 | 14.2 ± 12.0 | <0.01 |
| Success rate n (%)$^{\dagger}$ | 178 (98.9) | 176 (96.2) | 0.09 |
| Recurrence (%) | 3 (1.7) | 11 (6.3) | 0.02 |

AFL = atrial flutter; BMI = body mass index; CTI = cavotricuspid isthmus; MDCT = multidetecter computed tomography; RF = radiofrequency.
*Data given as mean and standard deviation.
$^{\dagger}$The procedural success rate was defined as bidirectional block after the RF ablation of the CTI.

the ablation catheter.[17,18] Scavée *et al*. demonstrated higher efficacy of an externally irrigated tip ablation catheter for rapid achievement of CTI block compared with an 8 mm tip catheter.[19] In contrast, the 8 mm tip catheter was demonstrated to be more effective for ablation in the case of a straight isthmus morphology where a constant high-blood flow is obtained compared with irrigated catheters.[20] Further, the stratified CTI morphology ("straight," "concave," and "pouch-like") included mostly the straight type in this study. Therefore, we used an 8 mm tip catheter throughout the study. The usefulness of a voltage-guided technique to target the high-voltage electrograms along the CTI to ablate the functionally important anatomical muscle bundles was reported recently.[21,22] The results of this study may be useful for overcoming difficult cases with this approach. When the catheter contact is poor, the catheter inversion technique will be necessary to map the target electrograms. Various imaging modalities (e.g., right atrial angiography, 3D mapping system, intracardiac echocardiography) have been utilized to characterize the CTI morphology and improve the AFL ablation procedure.[20,23,24] MDCT has the advantage of providing views of the CTI anatomy from every angle, and allows

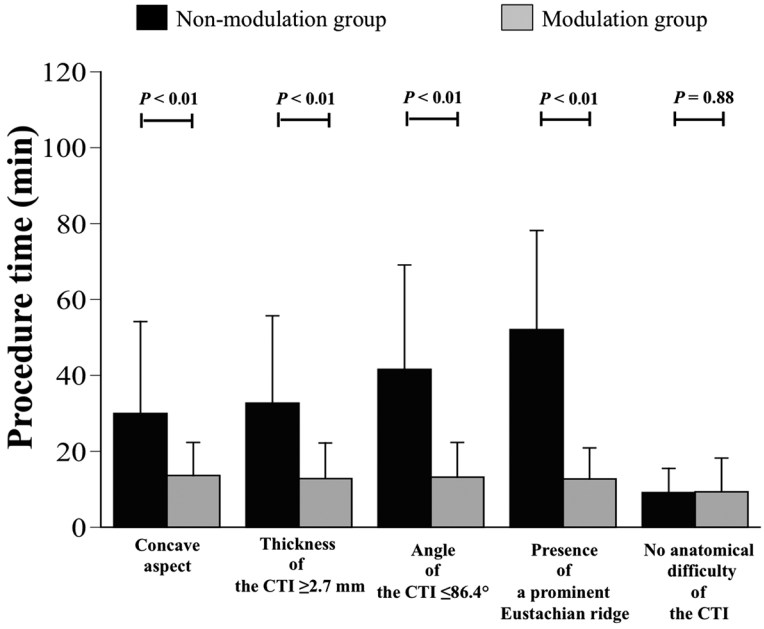


**Figure 4.** *Comparison of the procedure time between the modulation and nonmodulation groups according to the anatomical characteristics. The vertical bars represent minutes for the procedure time in this study.*

accurate measurements of the parameters of the CTI compared with the other imaging modalities.

### *Study Limitations*

This was a single-center study. Patients with extreme right atrial enlargement and hemodynamic factors such as severe tricuspid regurgitation or pulmonary hypertension were not included among the study subjects. Those factors may cause difficulty during ablation procedures. No mechanical valve replacements, pacemakers, or implantable cardioverter defibrillators were implanted in any of the patients included in our study because of the artifact interference during the analysis of the MDCT images. Only an 8 mm tip ablation catheter and shaped sheath were used for the ablation and we did not perform a comparison with other catheters, including contact sensing irrigated catheters, when investigating the effectiveness of the various procedural strategies. Use of different catheters and sheaths may therefore result in different outcomes for CTI ablation.[25]

A high output, high-temperature setting, and strong contact using the catheter inversion technique (modulation strategies) was not attempted in every case in this study. Modulation strategies may make accomplishment of CTI block easy in any case, but increase the risk of cardiac injury especially in a thin right atrium near the IVC region.

## Conclusion

An MDCT scan with a contrast injection provides an accurate method for preoperative evaluation of the highly variable anatomy of the CTI. Variable catheter ablation strategies based on the MDCT findings significantly improved the adaptation of the ablation catheter to the anatomical characteristics associated with the procedural difficulties with the CTI ablation compared with the conventional strategy. However, we have to consider that the additional exposure from the MDCT may be detrimental to the patients. Our point was not that all patients had better undergo preprocedural MDCT before the CTI ablation. The current results suggest that if we encounter challenging cases of a CTI ablation and cannot complete the CTI block by the usual conventional strategy, we can give thought to these anatomical difficulties and promptly shift to change the strategy. If no widespread double potentials or a decrease in the local electrogram is encountered in spite of sufficient electrode-tissue contact, we have to consider that the myocardial wall of the CTI wall is thick and should adjust the RF power output accordingly. If the RF power suddenly drops at a site, the ablation catheter may be positioned in the low blood flow area such as a pouch. In that case, we had better consider changing the location of the ablation line. In cases in whom complete bidirectional conduction block of the CTI cannot be achieved despite universal widespread double potentials along the CTI line, the electrode-tissue contact may be insufficient in the proximal part of the CTI. In those cases, the catheter inversion technique is useful and recommended.

*Acknowledgments:* The authors thank Masao Kiguchi, R.T., Department of Radiology, for his excellent technical assistance.

## References

1. Cheng J, Cabeen WR Jr, Scheinman MM: Right atrial flutter due to lower loop reentry: Mechanism and anatomic substrates. Circulation 1999;99:1700-1705.
2. Cosio FG, Lopez-Gil M, Goicolea A, Arribas F, Barroso JL: Radiofrequency ablation of the inferior vena cava-tricuspid valve isthmus in common atrial flutter. Am J Cardiol 1993;71:705-709.
3. Yang Y, Varma N, Keung EC, Scheinman MM: Reentry within the cavotricuspid isthmus: An isthmus dependent circuit. Pacing Clin Electrophysiol 2005;28:808-818.
4. Kirkorian G, Moncada E, Chevalier P, Canu G, Claudel JP, Bellon C, Lyon L, Touboul P: Radiofrequency ablation of atrial flutter. Efficacy of an anatomically guided approach. Circulation 1994;90:2804-2814.
5. Yang Y, Varma N, Keung EC, Scheinman MM: Reentry within the cavotricuspid isthmus: An isthmus dependent circuit. Pacing Clin Electrophysiol 2005;28:808-818.
6. Anselme F, Saoudi N, Poty H, Douillet R, Cribier A: Radiofrequency catheter ablation of common atrial flutter: Significance of palpitations and quality-of-life evaluation in patients with proven isthmus block. Circulation 1999;99:534-540.

7. Poty H, Saoudi N, Abdel Aziz A, Nair M, Letac B: Radiofrequency catheter ablation of type 1 atrial flutter. Prediction of late success by electrophysiological criteria. Circulation 1995;92:1389-1392.
8. Heidbüchel H, Willems R, van Rensburg H, Adams J, Ector H, Van de Werf F: Right atrial angiographic evaluation of the posterior isthmus: Relevance for ablation of typical atrial flutter. Circulation 2000;101:2178-2184.
9. Knecht S, Castro-Rodriguez J, Verbeet T, Damry N, Morissens M, Tran-Ngoc E, Peperstraete B, Tatnga V, Elkholti M, Decoodt P: Multidetector 16-slice CT scan evaluation of cavotricuspid isthmus anatomy before radiofrequency ablation. J Interv Card Electrophysiol 2007;20:29-35.
10. Saremi F, Pourzand L, Krishnan S, Ashikyan O, Gurudevan SV, Narula J, Kaushal K, Raney A: Right atrial cavotricuspid isthmus: Anatomic characterization with multi-detector row CT. Radiology 2008;247:658-668.
11. Kitagawa T, Yamamoto H, Ohhashi N, Okimoto T, Horiguchi J, Hirai N, Ito K, Kohno N: Comprehensive evaluation of noncalcified coronary plaque characteristics detected using 64-slice computed tomography in patients with proven or suspected coronary artery disease. Am Heart J 2007;154:1191-1198.
12. Tai CT, Haque A, Lin YK, Tsao HM, Ding YA, Chang MS, Chen SA: Double potential interval and transisthmus conduction time for prediction of cavotricuspid isthmus block after ablation of typical atrial flutter. J Interv Card Electrophysiol 2002;7:77-82.
13. Yamabe H, Okumura K, Misumi I, Fukushima H, Ueno K, Kimura Y, Hokamura Y: Role of bipolar electrogram polarity mapping in localizing recurrent conduction in the isthmus early and late after ablation of atrial flutter. J Am Coll Cardiol 1999;33:39-45.
14. Iesaka Y, Takahashi A, Goya M, Yamane T, Tokunaga T, Amemiya H, Fujiwara H, Nitta J, Nogami A, Aonuma K, Hiroe M, Marumo F, Hiraoka M: High energy radiofrequency catheter ablation for common atrial flutter targeting the isthmus between the inferior vena cava and tricuspid valve annulus using a super long tip electrode. Pacing Clin Electrophysiol 1998;21:401-409.
15. Poty H, Saoudi N, Nair M, Anselme F, Letac B: Radiofrequency catheter ablation of atrial flutter. Further insights into the various types of isthmus block: Application to ablation during sinus rhythm. Circulation 1996;94:3204-3213.
16. Shah DC, Takahashi A, Jais P, Hocini M, Clementy J, Haissaguerre M: Local electrogram-based criteria of cavotricuspid isthmus block. J Cardiovasc Electrophysiol 1999;10:662-669.
17. Sporton SC, Davies DW, Earley MJ, Markides V, Nathan AW, Schilling RJ: Catheter inversion: A technique to complete isthmus ablation and cure atrial flutter. Pacing Clin Electrophysiol 2004;27:775-778.
18. Wieczorek M, Djajadisastra I, Hoeltgen R: Catheter inversion to achieve complete isthmus block in patients with typical atrial flutter. Z Kardiol 2005;94:674-678.
19. Scavée C, Jaïs P, Hsu LF, Sanders P, Hocini M, Weerasooriya R, Macle L, Raybaud F, Clementy J, Haïssaguerre M: Prospective randomised comparison of irrigated-tip and large-tip catheter ablation of cavotricuspid isthmus-dependent atrial flutter. Eur Heart J 2004;25:963-969.
20. Da Costa A, Romeyer-Bouchard C, Dauphinot V, Lipp D, Abdellaoui L, Messier M, Thévenin J, Barthélémy JC, Isaaz K: Cavotricuspid isthmus angiography predicts atrial flutter ablation efficacy in 281 patients randomized between 8 mm- and externally irrigated-tip catheter. Eur Heart J 2006;27:1833-1840.
21. Lewalter T, Lickfett L, Weiss C, Mewis C, Spencker S, Jung W, Haverkamp W, Schwacke H, Deneke T, Proff J, Dorwarth U, Bauer W: "Largest amplitude ablation" is the optimal approach for typical atrial flutter ablation: A subanalysis from the AURUM 8 study. J Cardiovasc Electrophysiol 2012;23:479-485.
22. Jacobsen PK, Klein GJ, Gula LJ, Krahn AD, Yee R, Leong-Sit P, Mechulan A, Skanes AC: Voltage-guided ablation technique for cavotricuspid isthmus-dependent atrial flutter: Refining the continuous line. J Cardiovasc Electrophysiol 2012;23:672-676.
23. Chang SL, Tai CT, Lin YJ, Ong MG, Wongcharoen W, Lo LW, Chang SH, Hsieh MH, Chen SA: The electroanatomic characteristics of the cavotricuspid isthmus: Implications for the catheter ablation of atrial flutter. J Cardiovasc Electrophysiol 2007;18:18-22.
24. Scaglione M, Caponi D, Di Donna P, Riccardi R, Bocchiardo M, Azzaro G, Leuzzi S, Gaita F: Typical atrial flutter ablation outcome: Correlation with isthmus anatomy using intracardiac echo 3D reconstruction. Europace 2004;6:407-417.
25. Matsuo S, Yamane T, Tokuda M, Date T, Hioki M, Narui R, Ito K, Yamashita S, Hama Y, Nakane T, Inada K, Shibayama K, Miyanaga S, Yoshida H, Miyazaki H, Abe K, Sugimoto K, Taniguchi I, Yoshimura M: Prospective randomized comparison of a steerable versus a non-steerable sheath for typical atrial flutter ablation. Europace 2010;12:402-409.